

Changes in the Steinmetz Coefficients of Punched Soft-Magnetic Sheets

Original

Changes in the Steinmetz Coefficients of Punched Soft-Magnetic Sheets / Gmyrek, Zbigniew; Szulakowski, Jacek; Vaschetto, Silvio; Cavagnino, Andrea. - (2022), pp. 1-7. (2022 IEEE Energy Conversion Congress and Exposition (ECCE) Detroit, MI, USA 09-13 October 2022) [10.1109/ECCE50734.2022.9947908].

Availability:

This version is available at: 11583/2978933 since: 2023-05-30T13:16:47Z

Publisher:

IEEE

Published

DOI:10.1109/ECCE50734.2022.9947908

Terms of use:

This article is made available under terms and conditions as specified in the corresponding bibliographic description in the repository

Publisher copyright

IEEE postprint/Author's Accepted Manuscript

©2022 IEEE. Personal use of this material is permitted. Permission from IEEE must be obtained for all other uses, in any current or future media, including reprinting/republishing this material for advertising or promotional purposes, creating new collecting works, for resale or lists, or reuse of any copyrighted component of this work in other works.

(Article begins on next page)

Changes in the Steinmetz Coefficients of Punched Soft-Magnetic Sheets

Zbigniew Gmyrek

Institute of Mechatronics and Information Systems

Lodz University of Technology

Lodz, Poland

zbigniew.gmyrek@p.lodz.pl

Jacek Szulakowski

Institute of Mechatronics and Information Systems

Lodz University of Technology

Lodz, Poland

jacek.szulakowski@p.lodz.pl

Silvio Vaschetto

Senior Member, IEEE

Dipartimento Energia

Politecnico di Torino

Torino, Italy

silvio.vaschetto@polito.it

Andrea Cavagnino

Fellow, IEEE

Dipartimento Energia

Politecnico di Torino

Torino, Italy

andrea.cavagnino@polito.it

Abstract—This paper presents the measurement and numerical simulation results related to the iron loss components occurring in lamination sheets used to build cores of *ac* electric motors. The research is focused on the analysis of changes in the Steinmetz coefficients describing the material iron loss, as a function of the distance from the cut edge. The authors used an ad-hoc FEM model that takes into account the changes in the magnetic permeability and electrical conductivity of the material, which are a consequence of the used cutting technology. The analysis has been performed for three commercially available low-loss magnetic laminations having a thickness of 0.35 mm.

Keywords—Soft magnetic material, losses, punching process, damaged area, finite-element method (FEM), noninvasive measurements, Steinmetz coefficients.

I. INTRODUCTION

The impact of technological processes on the properties of magnetic laminations used to build cores of electric motors has been the focus of many studies over the years. In this research field, the literature reports several papers about modeling the magnetic permeability variation on the area lying close to the cut edge of punched lamination sheets [1]-[4]. Indeed, the deterioration of the magnetic characteristics on the lamination edge results in: *i*) a reduction in the magnetic induction averaged over the cross-section of the sheet for each magnetic field intensity, and *ii*) an increase or decrease in the averaged specific iron loss of the investigated material, depending on the magnetic field intensity. The research works in literature quite well address the modelling of these phenomena, both for punched and laser cut lamination sheets. However, how damaged zones on lamination edges impact the Steinmetz equation commonly used to compute the iron loss is still an open research topic.

For sinusoidal variation of the magnetic induction, the original form of Steinmetz equation in (1) can be used, where f is the frequency, B is the amplitude of magnetic induction, while k , a and b are coefficients dependent on the considered material.

$$P = k \cdot f^a \cdot B^b \quad (1)$$

Of particular importance is the analysis of the coefficients in (1) in relation to the two loss components: hysteresis loss and excess loss. Using the division into loss components proposed by Bertotti, the dependencies in (2) and (3) can be written for the hysteresis (P_h) and excess loss (P_{exc}) components.

$$P_h = k_h \cdot f \cdot B^{b_h} \quad (2)$$

$$P_{exc} = k_{exc} \cdot f^{1.5} \cdot B^{1.5} \quad (3)$$

In (2) and (3) b_h is the exponent of magnetic induction (i.e. the so-called Steinmetz exponent), k_h is the hysteresis loss coefficient, k_{exc} is the excess loss coefficient. The classical eddy current losses will be introduced and discussed in Section IV.A as the key quantity for an accurate determination of the Steinmetz coefficients.

The aim of this paper is to quantify the changes in the Steinmetz coefficients used in (1)-(3) as a function of the impact of the mechanical cutting process. For the purpose, the research work is based on non-invasive measurements carried out on rectangular samples of variable width from 4 mm to 60 mm made of three different soft magnetic materials having a thickness of 0.35 mm and subjected to a mechanical cutting process. Then, by combining the measurements with the FEM simulations and the results obtained from the developed analytical models, the variability of the Steinmetz coefficients was determined for the case of study.

The conducted research show that the main cause of changes in these coefficients is the existence of internal stresses caused by the used cutting technology. Indeed, it is known that the loss component related to hysteresis phenomenon is very sensitive to the presence of internal stress into the soft-magnetic material. On the other hand, researchers are divided over the effects of internal stress on excess losses. The research carried out investigating the low-loss grades of materials M300-35A, M270-35A and M235-35A, in the frequency range from 5 to 350 Hz, try to answer to this open questions.

II. RESEARCH STAND AND MEASUREMENT RESULTS

A. Measurements of Magnetic Properties

The conducted studies are based on the initial experimental assessment of multiple soft-magnetic lamination strips having different width. In detail, each sample was subjected to a punching process, and then analyzed for changes in material properties, such as magnetic permeability and specific iron loss. Measurements were made using an automated MAG-HT measuring system (a customized apparatus produced by R&J Measurement, Poland), adapted to test rectangular strips having a width in the range 4-60 mm.

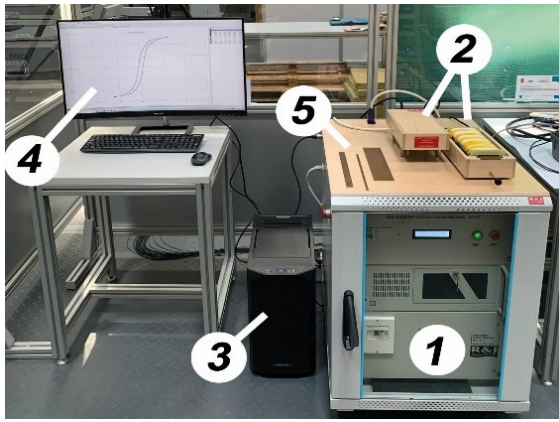


Fig. 1. Automated MAG-HT measuring system: 1 – power electronic module, 2 – measurement yoke, 3 – computer with a measuring and analyzing system, 4 – output display, 5 – tested lamination strips.

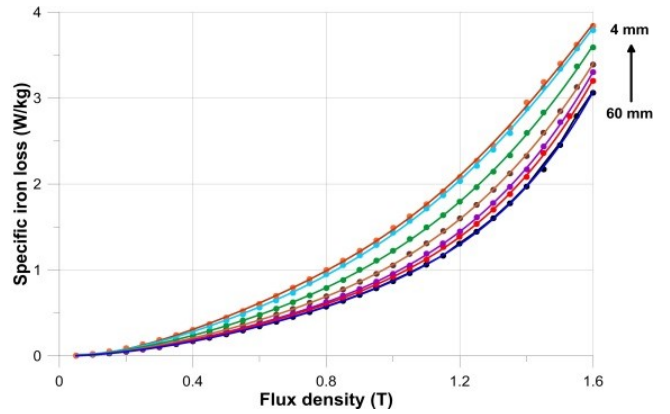
The variable width specimens tested for this research activity have a length equal to 300 mm and were produced considering a cut angle equal to 0 degrees in relation to the rolling direction of the sheet. Nevertheless, previous research activities conducted by the authors revealed a limited impact on the magnetization characteristics of the cutting angle with respect to the rolling direction [5]. For strips narrower than 60 mm, multiple samples have been tested at the same time in order to completely fill up the measurement yoke window (e.g. 12 strips having a width of 5 mm each were tested together).

Figure 1 shows the complete experimental setup, together with some samples of tested soft-magnetic lamination strips. The measuring systems can conduct tests at different frequency values in the range 5-350 Hz. The upper frequency value was chosen such that an even distribution of the induction amplitude within the cross section of the tested strip was ensured. The operation of the power electronic module is supervised by an algorithm that maintain the sinusoidal course of the magnetic flux density (within an accuracy of 1%) in the tested strips. The measuring apparatus is equipped with an automated sample demagnetizing system before each measurement. The measured data are saved in external files for post-processing analyses.

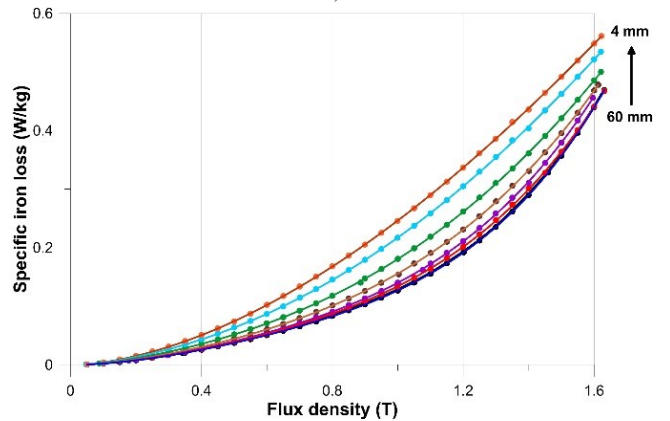
Figure 2 shows the specific iron loss versus the magnetic flux density measured for the M270-35A material at two different frequencies. For each width, the plotted results are average values over the strip cross-sections. The obtained trends well show that along with the reduction of the strips width, the induction exponent b that describes the iron losses according to (1) also reduces.

B. Measurements of Electrical Conductivity

The destruction of a part of the crystalline structure of the material during the punching process also impacts the electric properties of the soft-magnetic sheet, including its electrical conductivity. Such changes on the electrical conductivity can be observed using an appropriate four-wire measurement system. Figure 3 sketches the system layout used to measure the electric resistance of the different tested strips. In detail, a DC current of 100 mA was forced to flow in the system, and the voltage drop on a part of the strip length ($L = 0.25$ m) was measured with a FLUKE 8808A digital voltmeter.



a)



b)

Fig. 2. Measured specific iron loss for M270-35A lamination strips having width in the range 4-60 mm (a) at 50Hz; (b) at 10Hz

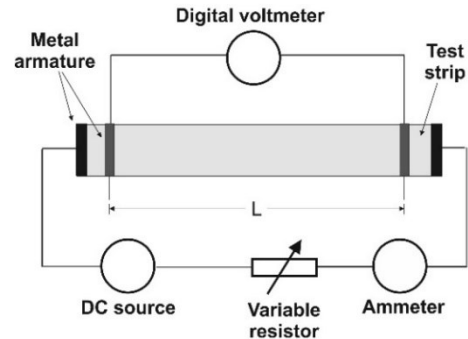


Fig. 3. Sketch of the system for measuring the electrical conductivity of the tested strip.

TABLE I AVERAGE ELECTRICAL CONDUCTIVITY MEASURED ON THE DIFFERENT STRIP WIDTHS FOR THE THREE TESTED MATERIALS

	Actual strip width (mm)						
	4	6	7.5	10	20	30	60
M300-35A, (MS/m)	1.97	2.01	2.03	2.03	2.03	2.04	2.04
M270-35A, (MS/m)	1.87	1.89	1.92	1.93	1.93	1.94	1.94
M235-35A, (MS/m)	1.46	1.50	1.51	1.51	1.51	1.52	1.52

Since the measured voltage values were in the orders of mV, a series of 10 measurements were made for each strip width, determining the average value of the resistance. Hence, using the well-known relationship between resistance, geometrical dimensions and electrical conductivity, the average values of electrical conductivity were determined for each strip separately.

Table I reports the average (per-cross section) electrical conductivity values measured on the variable width strip samples. The results obtained for the three investigated materials present similar conductivity variations versus the strip width, showing that for narrow strips the average electrical conductivity slightly reduces. This confirms that the deteriorated material close to the cutting edges impacts on the electrical properties of the material. The determined average electrical conductivities were then used to recreate the local conductivity values for damaged material zones in the FEM and analytical models used in the following parts of this research activity.

III. STEINMETZ COEFFICIENTS ANALYSIS FOR THE INVESTIGATED LAMINATIONS

To investigate the effective impact of the mechanical cutting process on the considered materials, a preliminary comparison between a punched strip and an ‘undamaged’ material sample has been conducted. In particular, water cutting technology is well recognized as one of the least invasive cutting techniques that only slightly changes the properties of the material close to the cut edge. Therefore, a water-cut strip 60 mm wide has been produced and considered as a baseline undamaged sample. For the investigated material grades, the specific iron losses measured for the undamaged and the punched strips having both a width of 60 mm are slightly different, reflecting in approximately 1% difference in the estimated Steinmetz exponents. The observed difference in the material properties can be related to the damaged material area that is present in the punched strip, while it is negligible in case of water jet cutting. Therefore, to investigate the changes in the Steinmetz coefficients because of the mechanical cutting process, a series of measurements were carried out on punched strips with a width of 4, 6, 7.5, 10, 20, 30 and 60 mm. The measurements were repeated at several frequencies in the range of 5-350 Hz to create a database for further analysis.

Sample results of the b_h exponent obtained for the different punched strip widths and flux density values are presented in Table II, Table III and Table IV for the three investigated materials. These exponents have been estimated by fitting the measurements at 5 Hz, where the hysteresis losses are the predominant components (typically around the 95-97% of the total losses). The results show that the variations of the Steinmetz exponents for the induction range 0-0.9 T are only a few percent, while for the range of 0.9-1.3 T they are in the order of 20 to 30%, and for the range of 1.3-1.6 T they reach even 45%, depending on the width of the tested strip. Generally, the smallest values of the b_h exponent are achieved for the narrowest strips under test. Once again, it is reminded that the results refer to the curves in which the induction and the specific loss were averaged over the strip cross section, considering in this way an equivalent change in material properties.

TABLE II - STEINMETZ EXPONENTS ESTIMATED AT 5 HZ FOR THE TESTED M300-35A MATERIAL

Strip width (mm)	Flux density range (T)		
	0 – 0.9	0.9 – 1.3	1.3 – 1.6
60	1.715	2.158	2.517
30	1.725	2.013	2.442
20	1.725	2.067	2.343
10	1.688	2.234	2.386
7.5	1.685	2.185	2.310
6	1.679	2.053	2.109
4	1.661	1.815	1.837

TABLE III - STEINMETZ EXPONENTS ESTIMATED AT 5 HZ FOR THE TESTED M270-35A MATERIAL

Strip width (mm)	Flux density range (T)		
	0 – 0.9	0.9 – 1.3	1.3 – 1.6
60	1.730	2.266	3.055
30	1.727	2.346	3.082
20	1.724	2.322	2.842
10	1.755	2.233	2.555
7.5	1.749	2.070	2.205
6	1.748	1.970	2.025
4	1.732	1.723	1.676

TABLE IV - STEINMETZ EXPONENTS ESTIMATED AT 5 HZ FOR THE TESTED M235-35A MATERIAL

Strip width (mm)	Flux density range (T)		
	0 – 0.9	0.9 – 1.3	1.3 – 1.6
60	1.729	2.008	2.693
30	1.790	2.063	2.517
20	1.746	2.197	2.630
10	1.706	1.942	2.445
7.5	1.667	1.918	2.028
6	1.608	1.774	1.817
4	1.590	1.543	1.519

As mentioned earlier, the change of Steinmetz coefficients in (1) can be related to the influence of internal stresses on the hysteresis and excess loss components. However, despite the tested materials have a very similar crystallographic structure, they feature slightly different electrical conductivities. In fact, typical values reported in catalogues for the investigated material grades are: 2 MS/m for the M300-35A, 1.92 MS/m for the M270-35, and 1.5 MS/m for the M235-35A. These variations reflect on different shares of eddy current losses, and thus a slightly different variability of the Steinmetz coefficients for the three considered materials. Therefore, the research activity has been focused on the analysis of the influence of the loss components on the Steinmetz coefficients.

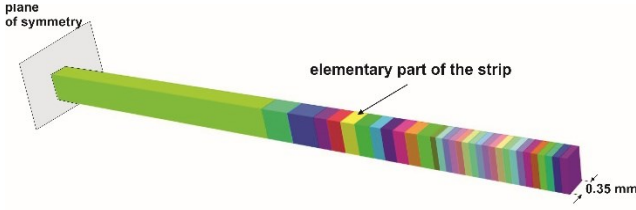


Fig. 4. The 3D FEM model of a punched soft-magnetic strip with 0.35 mm thickness. Colored elementary parts have different local material properties.

IV. ANALYSIS OF STEINMETZ COEFFICIENTS DESCRIBING THE COMPONENTS OF IRON LOSS

The next step in the research was to find the relationship between the iron loss components for a specific frequency and to check the range of their variability depending on the selected width of the strip and the specific induction level.

A. Loss component formulations

Generally known works of Bertotti's indicate the presence of three components of total iron loss: hysteresis loss described by (2), excess loss described by a simplified formula as in (3), and classical eddy current loss described by (4).

$$P_{class} = \frac{\pi^2 \gamma d^2 B_m^2 f^2}{6 \rho} \quad (4)$$

In (4), P_{class} is the classical eddy current loss density, γ is the electrical conductivity, d is the strip thickness, B_m is the amplitude of flux density, f is its frequency and ρ is the material density.

Taking into account changes in the electrical conductivity resulting from the destruction of the crystallographic structure of the material, the use of (4) is limited to strips having a width of more than 10 mm. In fact, the conducted measurements show that for punched strips larger than 10 mm the electrical conductivity is almost constant, independently on the strip width (see Table I). On the other hand, for narrow strips, the electrical conductivity value tends to reduce along with the strip width. In fact, for strips narrow than 10 mm, the various degrees of material destruction due to the punching process differently impact the material properties, depending on the distance from the cut edge. Hence, a constant electrical conductivity value valid for all strip widths cannot be considered in (4).

B. 3D FEM Model with Local Material Properties

To consider the changes in material properties as a function of the distance from the cut edge, the 3D FEM model shown in Fig. 4 has been developed. The figure highlights with different colors the elementary parts in which the model has been subdivided. For each elementary part, different local material properties have been applied to consider the different local magnetic permeability and electrical conductivity. In fact, the change in permeability is influenced by the damage to the grain structure (up to distances comparable to the thickness of the strips, i.e. 0.1-0.2 mm), and the presence of internal stresses (at a much greater distance, even up to several mm). Instead, the main causes for the electrical conductivity variation are the resulting dislocations and slips of the crystal structure present at up to several tenths of mm from the cut edge.

The necessity to take into account changes in electrical conductivity is already confirmed in literature [8]-[10]. As aforementioned, the magnetic permeability and the electrical conductivity measured on the punched strips are average values per strip cross section. Hence, the measured values represent equivalent physical quantities for each strip width. Nevertheless, each elementary part in which the FEM model has been subdivided requires local magnetic permeability and electric conductivity values. To get these local values, the analytical model discussed in [4] has been used to 'recreate' the local magnetic and electrical properties of the material in function of the distance from the cut edge.

In particular, the used analytical method is based on the measurement of the magnetic induction by means of a sensing coil covering the entire cross-section of the test strip. During the test, the magnetic flux generated by a primary coil winding penetrates the strip parallel to the cut edges, where some part of the material is damaged. As well known, damages due to the mechanical cutting process is not evenly spread through the strip cross section, but the closer to the cut edge, the greater the damage. The measurement done by the sensing coil comprises the total flux penetrating the strip, with a greater value in the undamaged part and a lower value in the damaged part. However, in the used measurement method, the total magnetic flux is divided by the cross-sectional area of the strip, determining the average value of the magnetic flux density. Therefore, the following formula can be written:

$$B_{av} = \frac{1}{S} \cdot \int_S B_i dS \quad (5)$$

where B_{av} is the measured average flux density, S is the strip cross-sectional area, B_i is the local (unknown) flux density, and dS is an elementary area. The previous equation can be rewritten as follow:

$$B_{av} = \frac{1}{S} \cdot \int_S \mu(x, H_i)_i H_i dS \quad (6)$$

where $\mu(x, H_i)_i$ is the local magnetic permeability (unknown) dependent on the x distance from cut edge and H_i is the magnetic field strength, that is assumed to be identical for each elementary area.

Based on several published research, it can be assumed that damages to the internal structure of the material due to the action of mechanical forces during cutting process causes a change in the local properties of the material. In particular, the changes in magnetic permeability or electrical conductivity can be approximated by using exponential curves [1], [6]-[7]. Therefore, in this study the authors consider the following relationship to describe the changes in magnetic permeability versus the distance from the strip cut edge:

$$\mu(x, H_i) = \mu_{nd}(H_i)(1 - e^{-ax}e^{-bH_i}) \quad (7)$$

where μ_{nd} is the magnetic permeability for the undamaged material, while a and b are curve fitting parameters. The local magnetic permeability curve described by (7) shows that, for x going to zero, the local permeability value tends to the measured mean value, while for x going to infinite the local magnetic permeability tends to the values of the undamaged material.

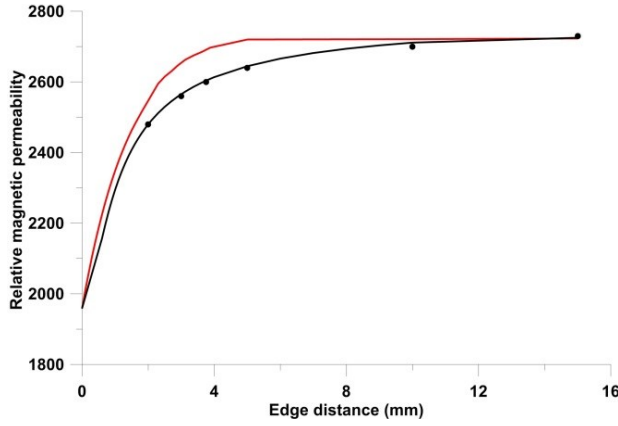


Fig. 5. Change in relative magnetic permeability of the punched material M300-35A at $H_{\max}=400$ A/m. Points: measurement results; black line: approximation of the average (measured) relative magnetic permeability; red line: approximation of local relative magnetic permeability by (7).

The local magnetic permeability values obtained by the analytical model (7) and applied to the different elementary parts of the FEM model are shown by the red curve in Fig. 5. The figure also reports in black the values obtained by the measurements on the variable width strips. The comparison highlights the non-negligible difference between the local quantities ‘reconstructed’ using the analytical approach with respect to the average (per strip cross sectional area) values obtained by measurements. As evident, for distances from the cut edge larger than 10 mm the curves overlaps, while for lower distances the average measured quantities lead the percentage error that increase up to several dozen percent.

Similarly, also the local values for the electrical conductivity were obtained using the measurements carried out and the method of recovering local material properties, proceeding in the same way as described for searching for local magnetic permeabilities. In particular, the changes in electrical conductivity versus the distance from the strip cut edge have been derived using the following relationship:

$$\gamma(x) = \gamma_{nd} \cdot (1 - b \cdot e^{-ax}) \quad (8)$$

where γ_{nd} is the electrical conductivity for undamaged material, a and b are fitting parameters, and x is the distance from the cut edge. Figure 6 shows the analytically ‘reconstructed’ local values of the electrical conductivity for the M300-35A material, together with the measured (average) quantities.

C. Determination of the loss components

The developed 3D FEM model made it possible to take into account the local properties of the material, which made it possible to precisely determine the classical eddy current losses. As expected, for strips with a width larger than 10 mm, the calculation of this loss component according to (4) practically coincided with the results from the 3D FEM model. Besides, the smaller the width of the strip, the greater the difference. For example, for a strip with a width of 4 mm, the classical eddy current loss component calculated by the 3D FEM model was approximately 9% lower than that calculated according to (4), for the same average induction in the strip cross-section.

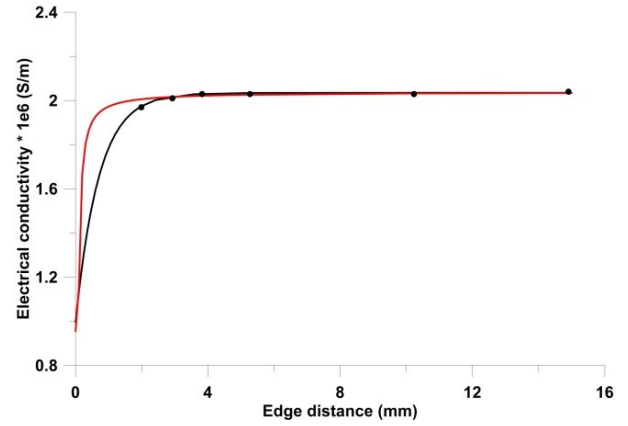


Fig. 6. Change in electrical conductivity of the punched material M300-35A. Points: measurement results; black line: approximation of the average (measured) electrical conductivity; red line: approximation of local electrical conductivity by (8).

TABLE V - THE VALUES OF THE k_h AND k_{exc} COEFFICIENTS DETERMINED AT 1T FOR THE THREE INVESTIGATED MATERIALS

Strip width (mm)	Material type					
	M300-35A		M270-35A		M235-35A	
	k_h (*)	k_{exc} (*)	k_h (*)	k_{exc} (*)	k_h (*)	k_{exc} (*)
4	215	9.19	229	12.45	160	12.69
6	185	7.44	167	9.67	133	10.27
7.5	161	7.1	145	9.02	110	9.95
10	147	6.75	123	8.27	104	9.41
20	142	6.54	108	6.74	93	8.20
30	139	6.37	103	6.70	87	7.89
60	132	5.65	101	6.68	79	7.57

(*) k_h and k_{exc} values listed in the table have to be multiplied by $1e-4$.

The precise determination of the eddy current losses enabled the accurate analysis also of the remaining iron loss components, thus explaining the change in the Steinmetz exponents presented in Tables II-IV for the three investigated materials. To evaluate the total iron loss P_{iron} and the different iron loss components, the simplified relationship in (9) can be used instead of the original Bertotti’s formulation. In (9) the $k_{exc}(B)$ takes into account the dependence of the excess losses by the flux density raised to 1.5.

$$\frac{P_{iron}}{f} = k_h B^{b_h} + \frac{P_{class}}{f} + k_{exc}(B) \cdot f^{0.5} \quad (9)$$

By the measurement of the total iron loss and the knowledge of classical eddy current loss calculated using the above described approach, the k_h , b_h and k_{exc} coefficients were determined for the individual strip widths and induction levels using the least squares method. The search was carried out for the three tested materials, using the results of measurements carried out for frequencies ranging from 5 to 350 Hz. First, the values of the k_h and k_{exc} coefficients were determined for an induction equal to 1 T. The parameter k_h determined in this way was the basis for finding the exponent b_h , assuming at this stage that the parameter k_h does not depend on the induction level.

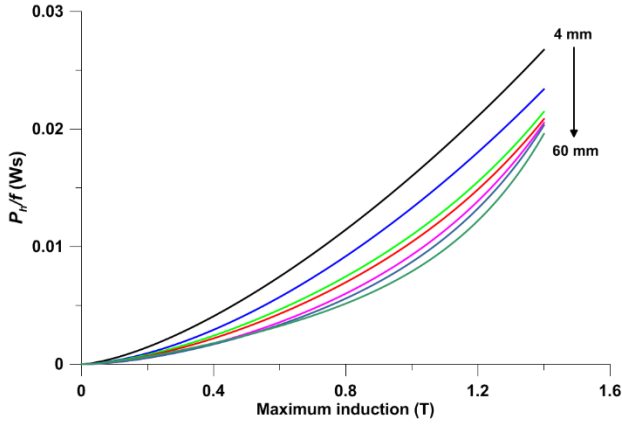


Fig. 7. Change in P_h/f vs. maximum induction for the tested M235-35A material punched in strips having variable width.

The values of the k_h and k_{exc} parameters, relating to the loss density in W/kg, determined for the three tested materials and the 1 T induction are reported in Table V. The obtained results show that as the proportion of damaged material increases (i.e. reducing the strips width) the hysteresis and excess losses increase as well. In particular, for a strip width reduction from 60 mm down to 4 mm, the increase in hysteresis losses resulted equal to 63%, 127% and 103%, respectively, for the materials M300-35A, M270-35A and M235-35A. The excess loss increase is 63%, 86% and 68%, respectively.

Once k_h and k_{exc} coefficients were defined, the variability of the b_h exponent in (2) was analyzed, assuming that for any magnetic induction value B_{av} the coefficient k_h is constant and equal to the value previously determined at 1 T. Based on this assumption, it is therefore possible to write (2) as in (10).

$$P_h = k_h(1 T) \cdot f \cdot B_{av}^{b_h} \quad (10)$$

Similarly, the excess losses can be determined for any induction B_{av} assuming a constant value for the coefficient k_{exc} . Also for this loss contribution, the material coefficient value determined at 1 T has been considered constant; consequently, it is possible to write the following formulation:

$$P_{exc} = k_{exc}(1 T) \cdot f^{1.5} \cdot B_{av}^{b_{exc}} \quad (11)$$

where b_{exc} is the induction exponent in excess loss part.

An example of the variability of the P_h/f and b_h exponents as a function of the strip width and B_{av} induction are shown in Fig. 7 and Fig. 8, respectively. It should be emphasized that the nature of the changes is very similar for each type of material tested.

During the research it was found that the exponent of the power b_{exc} in (11) depends on the degree of material destruction and the level of induction. For narrow strips it is almost independent from the induction and approximately equal to 1.5 in accordance to the Bertotti's theory. For wider strips, the obtained results show that it becomes dependent on the level of induction as well as the width of the strip. Further investigations are ongoing to have a clearer view on the variation of the b_{exc} exponent.

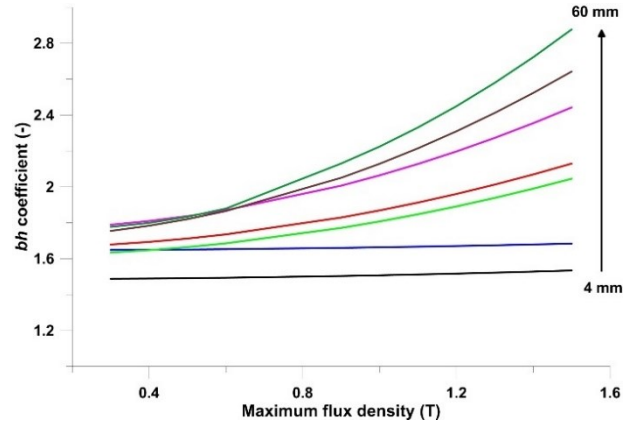


Fig. 8. Change in b_h coefficient at $k_h(1 T) = const$ vs. maximum induction for the tested M235-35A material punched in strips having variable width.

V. DISCUSSION

Similar studies carried out by other research groups indicate the achievement of similar increases in specific iron loss, although they do not conduct such an in-depth analysis of the loss components [11]. The main impact of the punching, grain size deformation and internal stresses on the change in the value of the indicated loss components is also confirmed by other researchers, although their works concern the general problem without taking into account the impact of the cutting process [12].

The problem of numerical analysis of changes in hysteresis losses due to the cutting process, taking into account the profiles of changes in material properties near the cut edge, was analyzed by another group of researchers [13]. They found results in line with those presented in this study, including a change in eddy-current, hysteresis and excess losses. Moreover, the values of the b_h exponent obtained as a result of the conducted analysis are within the limits described in the literature [14].

For relatively low frequencies, i.e. 50-350 Hz, the observed increase in loss along with the decrease in the width of the strips can be explained primarily by a large share of hysteresis losses (e.g. for 200 Hz the hysteresis losses constitute about 50% of the total losses). For higher frequencies, i.e. in the order of kHz, the observed loss increases cannot be explained by this reason, due to a much smaller share of hysteresis losses. This can be explained by the significant proportion of excess loss which has also been shown to increase in value as the width of the strips decreases. Work in this area, using the formula of loss components proposed by Bertotti, indicating the need to take into account the increase in excess losses also at frequencies of hundreds of Hz, was carried out by another group of researchers [15]. The conclusions resulting from the current works and those indicated in [13] are similar.

A separate problem is the use of the conducted research to find local increases in loss components, as well as the preservation of the magnetic induction exponent in the Bertotti's relation describing the excess losses - the value proposed by Bertotti is 1.5. In the literature we can find works showing that assuming a constant value of the exponent equal to 1.5, an increase in excess losses is noticeable.

However, these works do not answer the question whether the material coefficient present in the equation describing this loss component is constant or changes with the level of induction and degradation [16]. The authors indicate that it is possible to change the value of the exponent along with the level of induction and the degree of material destruction. A discussion on the variability of the Steinmetz coefficients resulting from the adoption of specific dependencies representing the components of losses can be found in [17] that partially confirms the results described here.

VI. CONCLUSION

The article presents the results of measurements obtained for three low-loss soft magnetic laminated materials subjected to punching process. In particular, the research work investigates the variation of the Steinmetz coefficients and core loss components in function of the distance from the lamination cut edge. For each investigated material, measurements conducted on strips having variable width in the range 4-60 mm have been supplemented with numerical analyses performed with a 3D FEM model that has been properly developed to take into account the magnetic material degradation along with the distance from the cut edge. The local changes in magnetic permeability and electrical conductivity for the damaged material have been derived from analytical models reported in literature.

The obtained results show that the destruction of the grain structure and the presence of internal stresses, resulting from the applied mechanical cutting technology, cause changes not only in hysteresis losses, but also in excess losses. It has been shown that the increase in hysteresis loss for the test strips can be up to about 130% with respect to the loss for the undamaged material, and the increase in excess loss can reach approximately 90%. The conducted in-depth research work confirms the loss component variation indicated by other researchers. On the other hand, the changes on the Steinmetz coefficients in function of the material degradation only finds partial confirmation in literature, and still require additional investigations. Additionally, in the future also other cutting technologies will be investigated (i.e the laser cutting) to extend the knowledge on the variation of the Steinmetz coefficients.

ACKNOWLEDGMENT

The research conducted by Z. Gmyrek and J. Szulakowski was funded by the National Science Center (NCN) Poland as part of the “Opus –18”, Grant Number 2019/35/B/ST8/00764 “The manufacturing technology impact analysis of small- power high-speed electric motors to refine their analytical models”.

REFERENCES

- [1] L. Vandebossche, S. Jacobs, F. Henrotte, K. Hameyer, “Impact of cut edges on magnetization curves and iron losses in e-machines for automotive traction,” *World Electr. Veh. J.*, vol. 4, pp. 587–596, 2010.
- [2] M. Bali, H. De Gersem and A. Muetze, “Finite-element modeling of magnetic material degradation due to punching”, *IEEE Trans. Magn.*, vol. 50, 7018404, 2014.
- [3] R. Sundaria, A. Lehtikoinen, A. Arkkio, A. Hannukainen, “Higher-order finite element modeling of material degradation due to cutting”, in *IEEE-IEMDC*, 2017, pp. 1-7.
- [4] Z. Gmyrek, “Impact of a punching process on the SyRM iron loss: SPICE model as an effective tool for iron loss modeling,” *Energies*, 14, 7185, pp. 1-19, 2021.
- [5] M. Dems, K. Komez, Z. Gmyrek, J. Szulakowski, “The effect of sample’s dimension and cutting technology on magnetization and specific iron losses of FeSi laminations” *Energies*, 15, 2086, pp. 1-22, 2022.
- [6] R. Sundaria, A. Lehtikoinen, A. Arkkio, A. Hannukainen, “Higher-order finite element modeling of material degradation due to cutting”, *IEEE-IEMDC* 2017, pp. 1–7, 2017.
- [7] M. Bali, H. De Gersem, A. Muetze, “Finite-element modeling of magnetic material degradation due to punching”, *IEEE Trans. Magnetics*, vol.50, 7018404, 2014.
- [8] S. Xie, L. Wu, Z. Tong, H. Chen, T. Uchimoto, T. Takagi, “Influence of plastic deformation and fatigue damage on electromagnetic properties of 304 austenitic stainless steel”, *IEEE Trans. Magnetics*, vol.54, no8, 62001710, 2018.
- [9] A. Daem, P. Sergeant, L. Dupre, S. Chaundhuri, V. Bliznuk, L. Kestens, “Magnetic properties of silicon steel after plastic deformation”, *Materials*, 13, 4361, 2020.
- [10] F. Zhang, H. Li, C. Zhao, R. Jia, “Effect model of stress and plastic deformation on conductivities of various magnetic materials”, *IEEE Access*, vol.8, 82741, 2020.
- [11] R. Sundaria, A. Daem, A. Hemeida, P. Sergeant, A. Arkkio, A. Belahcen, “Effect of different cutting techniques on magnetic properties of grain oriented steel sheets and axial flux machines”, *IECON 2019 - 45th Annual Conference of the IEEE Industrial Electronics Society*, 2019.
- [12] H. Naumoski, A. Maucher, U. Herr, “Investigation of the influence of global stresses and strains on the magnetic properties of electrical steels with varying alloying content and grain size”, *Proc. 5th EDPC conference*, 2015.
- [13] S. Elfgen, P. Rasilo, K. Hameyer, “Hysteresis and eddy-current losses in electrical steels utilising edge degradation due to cutting effects”, *Int. J. Numer. Model.*, 33, e2781, pp.1-10, 2020.
- [14] J. Reinert, A. Broekmeyer, W.A. De Doncker Rik, “Calculation of losses in ferro- and ferrimagnetic materials based on the modified Steinmetz equation”, *IEEE Trans. Ind. Appl.*, vol.37, no.4, pp.1055-1061, 2001.
- [15] G. Paltanea, V. Manescu, R. Stefanoiu, I. Nemoianu and H. Gavrila, “Correlation between magnetic properties and chemical composition of non-oriented electrical steels cut through different technologies”, *Materials*, 13, 1455, pp.1-17, 2020.
- [16] A. Baghel, J. Blumenfeld, L. Santandrea, G. Krebs and L. Daniel, “Effect of mechanical stress on different loss components along orthogonal directions in electrical steels”, *Electrical Engineering*, no 3, 2019.
- [17] L. Petrescu, V. Ionita, E. Cazacu, and C. Petrescu, “Steinmetz’ parameters fitting procedure for the power losses estimation in soft magnetic materials”, *Proc. 2017 OPTIM & ACEMP Conference*, 2017.